Received: 7 December 2020 | Revised: 8 June 2021 | Accepted: 17 June 2021

DOI: 10.1111/cas.15035

ORIGINAL ARTICLE

Cancer Science WILEY

Trametinib overcomes *KRAS*-G12V–induced osimertinib resistance in a leptomeningeal carcinomatosis model of *EGFR*-mutant lung cancer

Koji Fukuda[1,2] | Sakiko Otani[1,3] | Shinji Takeuchi[1,2] | Sachiko Arai[1] | Shigeki Nanjo[1,4] | Azusa Tanimoto[1] | Akihiro Nishiyama[1] | Katsuhiko Naoki[3] | Seiji Yano[1,2]

[1]Division of Medical Oncology, Cancer Research Institute, Kanazawa University, Kanazawa, Japan

[2]Nano Life Science Institute, Kanazawa University, Kanazawa, Japan

[3]Department of Respiratory Medicine, Kitasato University School of Medicine, Kanagawa, Japan

[4]Department of Medicine, Division of Hematology-Oncology, University of California San Francisco, San Francisco, CA, USA

Correspondence
Koji Fukuda and Shinji Takeuchi, Division of Medical Oncology, Cancer Research Institute, Kanazawa University, 13-1 Takara-machi, Kanazawa, Ishikawa 920-0934, Japan.
Email: kfukuda@staff.kanazawa-u.ac.jp; takeuchi@staff.kanazawa-u.ac.jp

Funding information
Japan Society for the Promotion of Science, Grant/Award Number: 17K09649, 18K07261, 19H03665 and 20K17213

Abstract

Leptomeningeal carcinomatosis (LMC) occurs frequently in non–small cell lung cancer (NSCLC) harboring epidermal growth factor receptor (*EGFR*) mutations and is associated with acquired resistance to EGFR tyrosine kinase inhibitors (EGFR-TKIs). However, the mechanism by which LMC acquires resistance to osimertinib, a third-generation EGFR-TKI, is unclear. In this study, we elucidated the resistance mechanism and searched for a novel therapeutic strategy. We induced osimertinib resistance in a mouse model of LMC using an *EGFR*-mutant NSCLC cell line (PC9) via continuous oral osimertinib treatment and administration of established resistant cells and examined the resistance mechanism using next-generation sequencing. We detected the Kirsten rat sarcoma (*KRAS*)-G12V mutation in resistant cells, which retained the *EGFR* exon 19 deletion. Experiments involving *KRAS* knockdown in resistant cells and *KRAS*-G12V overexpression in parental cells revealed the involvement of *KRAS*-G12V in osimertinib resistance. Cotreatment with trametinib (a MEK inhibitor) and osimertinib resensitized the cells to osimertinib. Furthermore, in the mouse model of LMC with resistant cells, combined osimertinib and trametinib treatment successfully controlled LMC progression. These findings suggest a potential novel therapy against *KRAS*-G12V–harboring osimertinib-resistant LMC in *EGFR*-mutant NSCLC.

KEYWORDS
epidermal growth factor receptor, leptomeningeal carcinomatosis, non–small cell lung cancer, osimertinib, trametinib

Koji Fukuda and Sakiko Otani contributed equally to this article.

1 | INTRODUCTION

Central nervous system (CNS) metastases, such as brain metastases and leptomeningeal carcinomatosis (LMC), occur in 20%-40% of cancer patients.[1] CNS metastases induce various neurological symptoms, including headaches and hemiparesis, lower the quality of life, and are associated with poor prognosis. Various cancer types are characterized by CNS metastasis, the leading cause of which remains non–small cell lung cancer (NSCLC), followed by melanoma and renal and breast cancer.[1] Activating mutations in epidermal growth factor receptor (*EGFR*) are detected in ~10% of Caucasian and 50% of East Asian patients with lung cancer. CNS progression occurs in 15%-30% of patients treated with EGFR tyrosine kinase inhibitors (EGFR-TKIs) and is more frequent in patients with *EGFR* mutations than in those without such mutations.[2] LMC occurs in 3.4%-3.8% of NSCLC patients, with a higher frequency (9.4%) observed in patients with *EGFR* mutations.[3] Thus, controlling CNS metastasis is crucial for managing *EGFR*-mutant NSCLC.

The first-generation EGFR-TKIs gefitinib and erlotinib[3,4] are highly effective against *EGFR*-mutant NSCLC; however, recurrence occurs frequently in the CNS. The third-generation EGFR-TKI osimertinib specifically inhibits activated mutants and/or the *EGFR*-T790M resistance mutant but not wild-type *EGFR* or other kinases.[5] Osimertinib was initially approved for treating *EGFR*-T790M–positive NSCLC patients who acquired resistance to first- or second-generation EGFR-TKIs. Data from the FLAURA study showed that in patients with *EGFR*-mutated NSCLC, progression-free survival increased to a greater extent following treatment with first-line osimertinib than with gefitinib or erlotinib.[6] Therefore, first-line treatment with osimertinib has been approved as a standard therapy for patients with *EGFR*-mutated NSCLC.

Osimertinib shows efficacy against CNS metastases originating from *EGFR*-mutated NSCLC, with objective response rates and disease control rates in the CNS at 64% (95% confidence interval [CI], 53%-76%; n = 195) and 90% (95% CI, 85%-93%; n = 246), respectively.[7] However, osimertinib resistance causes recurrent CNS metastasis.[8] Moreover, an LMC patient reportedly acquired an *EGFR*-C797S mutation during osimertinib treatment.[9] Osimertinib resistance mechanisms involve the following: acquisition of an *EGFR*-C797S mutation; loss of the T790M mutation; activation of a bypass pathway involving mesenchymal-epithelial transition factor (MET), human epidermal growth factor receptor 2 (HER2), and Kirsten rat sarcoma (KRAS); and histological transformation, including small cell transformation[5] and epithelial-mesenchymal transition (EMT).[10] Although the resistance mechanisms in CNS metastasis are believed to reflect limited penetration of drugs into the CNS, the precise mechanisms remain unknown.

Here, we established an osimertinib-resistant cell line using a mouse model of LMC based on *EGFR*-mutant NSCLC following continuous oral osimertinib treatment and elucidated the mechanism underlying resistance development to identify novel therapeutic strategies.

2 | MATERIALS AND METHODS

2.1 | Cell culture and reagents

The *EGFR*-mutant human lung adenocarcinoma cell line PC9 (del E746_A750) was purchased from RIKEN Cell Bank. The H1975 human lung adenocarcinoma cell line with the *EGFR*-L858R/T790M double mutation was provided by Dr Yoshitaka Sekido (Aichi Cancer Center Research Institute). All cells were maintained in Roswell Park Memorial Institute (RPMI)-1640 medium supplemented with 10% fetal bovine serum (FBS), penicillin (100 U/mL), and streptomycin (10 μg/mL) in a humidified CO_2 incubator at 37°C. Osimertinib, rociletinib, and trametinib were obtained from Selleck Chemicals. Cell line authentication was performed using short tandem repeat analysis at the National Institute of Biomedical Innovation.

2.2 | Antibodies and Western blotting

Primary antibodies against EGFR, MET, phospho-MET (Y1234/Y1235), HER2, phospho-HER2 (Y1221/1222), Akt (Ak strain transforming), phospho-Akt (S473), E-cadherin, vimentin, cleaved caspase-3 (c-caspase-3), and β-actin were obtained from Cell Signaling Technology. Antibodies against extracellular signal–regulated MAP kinase (ERK)1/ERK2, phospho-ERK1/ERK2 (T202/Y204), and EGFR were obtained from R&D Systems. An anti-KRAS antibody was obtained from Santa Cruz Biotechnology. Western blot analysis was performed, as previously described.[11]

2.3 | Cell viability assay

Cells (2×10^3 cells/well) were seeded in 96-well plates in 100 μL RPMI-1640 containing 10% FBS, incubated for 24 hours, and then treated with osimertinib or rociletinib for 72 hours. Cell growth was measured using MTT (Sigma-Aldrich), as previously described.[11]

2.4 | *EGFR* mutation analysis

Cellular DNA was examined for *EGFR* mutations within exons 18 through 21 using the peptide nucleic acid–locked nucleic acid PCR clamp method.[12] The exon-19 mutation encoding the D761Y mutation was detected by DNA sequencing, as described previously.[13] The C797S mutation was detected by performing digital droplet PCR (ddPCR) using a Bio-Rad QX200 ddPCR instrument, as previously described.[11]

2.5 | C-caspase-3 assay

Cells (2×10^3 cells/well) were seeded in 96-well plates in 100 μL RPMI-1640 supplemented with 10% FBS, incubated for 24 hours, and treated with NucView 488 caspase-3 substrate (Biotium) and

then with osimertinib and/or trametinib for 24 hours. C-caspase-3 activity was observed using a fluorescence microscope (Nikon).

2.6 | siRNA transfection

siRNA oligonucleotides specific to *KRAS* were obtained from Dharmacon. A negative-control siRNA and siRNA specific to *EGFR* were purchased from Thermo Fisher Scientific. Cells were transfected with siRNAs using Lipofectamine RNAiMAX (Thermo Fisher Scientific) according to manufacturer instructions. Cells were detached and diluted in complete growth medium without antibiotics and then seeded into six-well plates (1×10^5 cells/well). RNAi duplex (final, 50 nM) and Lipofectamine RNAiMAX (9 mL) complexes were added to the wells containing the cells and medium (2 mL). The cells were incubated for 48 hours at 37°C and subsequently treated with alectinib. The siRNA sequences were as follows: si-EGFR, 5′-GAAUAGGUAUUGGUGAAUU-3′; and si-KRAS, which included a mixture of four siRNAs, including 5′-UACACAAAGAAAGCCCUCC-3′, 5′-UUACACACUUUGUCUUUGA-3′,5′-AAAGGAAUUCCAUAACUUC-3′, and 5′-AUACGCAUCGUGUUAUCUC-3′.

2.7 | Plasmid construction

Lentiviral vectors expressing human KRAS-G12V were purchased from Addgene. Lipofectamine LTX and PLUS reagent (Invitrogen) were used to transfect cells with the plasmids according to manufacturer instructions. PC9-ffluc and H1975 cells infected with the lentiviral vectors were continuously selected using hygromycin B (Wako Pure Chemical Co.). Lysates obtained from the selected cells were analyzed using Western blotting.

2.8 | Tumor cell transplantation in SHO-Prkdc^{scid}Hr^{hr} mice with severe combined immunodeficiency (SCID)

Six-week-old male SHO-Prkdc^{scid}Hr^{hr} mice (SHO-SCID mice) were obtained from Charles River Laboratories. To develop the leptomeningeal metastasis model, the scalp was sterilized with 70% ethanol, and cultured tumor cells (PC9-OR#2 harboring *KRAS*-G12V; 4×10^5 cells/0.1 mL) were injected into the leptomeningeal space (between the external occipital protuberance and the first cervical vertebra) using a 27-gauge needle. Tumor number in live mice was tracked by repeated noninvasive optical imaging using a tumor-specific luciferase assay and the IVIS Lumina XR imaging system (PerkinElmer). After 20 minutes, the luciferase substrate luciferin (150 mg/kg) was injected intraperitoneally. The mice were photographed under bright-field illumination, and the images were overlaid with luminescence data gathered between 1 and 30 seconds after the mice were anesthetized with 2% isoflurane. The bioluminescence signal intensity was analyzed, as previously described.[14] This study was performed in strict accordance with the recommendations of the Guide for the Care and Use of Laboratory Animals proposed by the Ministry of Education, Culture, Science, and Technology, Japan. The protocol was approved by the Committee on the Ethics of Experimental Animals and the Advanced Science Research Center, Kanazawa University, Kanazawa, Japan (approval no. AP-153499). All surgeries were performed on mice anesthetized using sodium pentobarbital, and efforts were made to minimize animal suffering.

2.9 | Immunohistochemistry

For immunohistochemistry of brain tissue samples, we used an HRP-based immunohistochemical detection system (EnVision+System-HRP, Rabbit [DAB+]). The antibody diluent and serum-free protein block were purchased from Dako/Agilent Technologies. Formalin-fixed paraffin-embedded brain tissue sections were subjected to antigen retrieval and endogenous peroxidase blocking, followed by incubation with the primary antibody overnight at 4°C. Subsequently, the slides were rinsed and incubated with a peroxidase-labeled polymer, rinsed, stained with the substrate-chromogen 3,3′-diaminobenzidine, and counterstained with Hematoxylin Gill I (EMD Millipore) and bluing reagent (EMD Millipore).

2.10 | Statistical analyses

A two-sided Student's *t*-test was used for intergroup comparisons. A $P < .05$ was considered significant.

3 | RESULTS

3.1 | Establishment of osimertinib-resistant *EGFR*-mutant lung cancer cells

To establish a mouse mode of LMC, we first injected *EGFR*-mutant lung cancer cells (PC9-ffluc) transiently expressing the luciferase gene into the leptomeningeal space of SHO mice, after which the mice were treated daily with 6 mg/kg osimertinib. After continuous treatment with osimertinib for 2 weeks, the LMC mice developed osimertinib resistance and were subsequently treated daily with 25 mg/kg osimertinib for 2 weeks. We successfully developed cell lines from three different mice: PC9-OR#1, PC9-OR#2, and PC9-OR#3. We then examined the sensitivity of selective EGFR inhibitors against the resistant cell lines. Resistance to osimertinib was >200-fold higher in all three cell lines than in the parental PC9-ffluc cell line (Figure 1A). Additionally, the cells showed cross-resistance to rociletinib. To elucidate the changes in EGFR status in the resistant cells, we examined EGFR expression and phosphorylation using Western blotting. Increased EGFR phosphorylation occurred in PC9-OR#2 cells, whereas EGFR expression decreased slightly in PC9-OR#2 and PC9-OR#3 cells (Figure 1B). Furthermore, osimertinib effectively

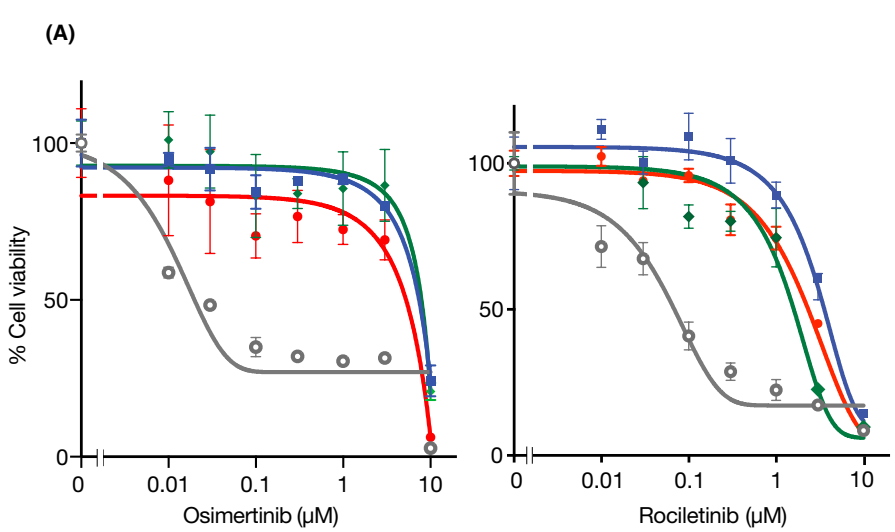

IC_{50} (μM)

Cells	Osimertinib	Rociletinib
PC9-ffluc	0.02	0.06
PC9-OR#1	7.75	1.61
PC9-OR#2	8.27	3.61
PC9-OR#3	5.42	2.34

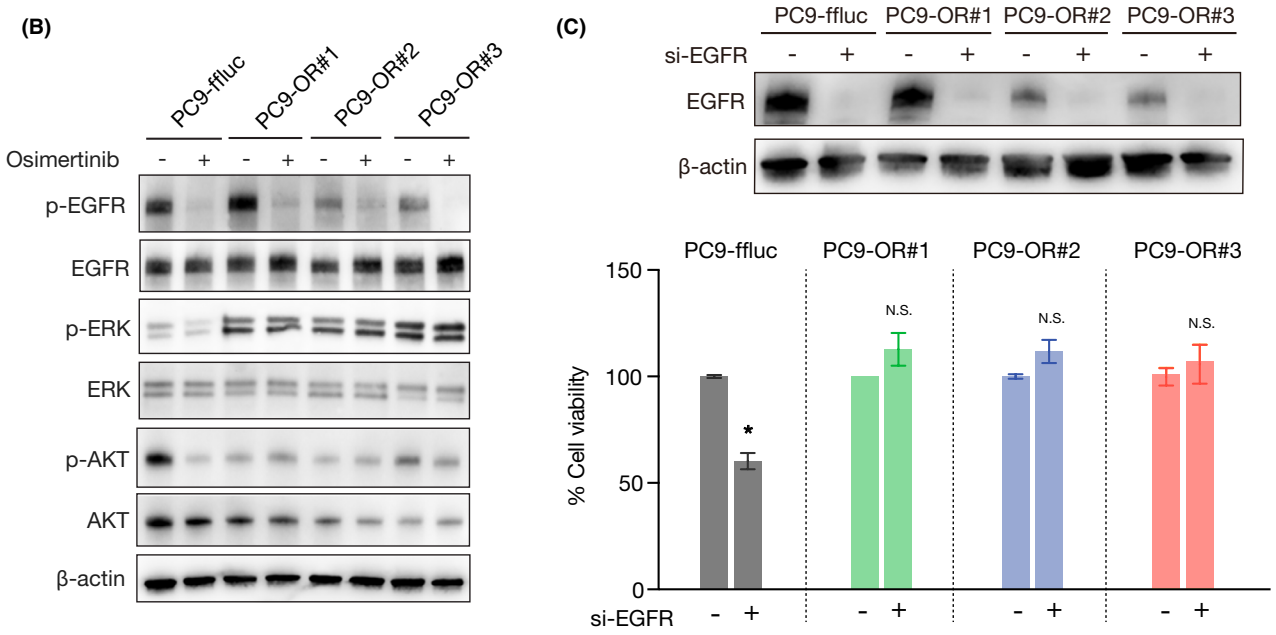

FIGURE 1 Generation of osimertinib-resistant PC9 cell clones in vivo. A, SHO mice were injected with PC9-ffluc cells in the leptomeningeal space. Next, the mice were daily treated with osimertinib. After continuous treatment with osimertinib for 4 wk, the mice developed leptomeningeal carcinomatosis (LMC) with acquired osimertinib resistance. MTT assays were performed to assess the growth inhibition of PC9-ffluc cells and the resistant clones, following treatment with osimertinib or rociletinib for 72 h (n = 3). The results are expressed as the mean ± standard error of the mean (SEM). The calculated IC_{50} values are shown. B, The parental PC9-ffluc cells and the resistant clones were treated with 1 μM osimertinib for 2 h. Changes in the phosphorylation levels of the indicated proteins were assessed by Western blotting. C, Control and epidermal growth factor receptor (EGFR) siRNAs were transfected into parental and resistant cells, and *EGFR* knockdown was confirmed by Western blotting. Cell viabilities were analyzed after 72 h by performing MTT assays (n = 3). *$P < .001$

inhibited EGFR phosphorylation in the parental PC9-ffluc cell line, as well as in the three resistant cell lines, whereas downstream ERK phosphorylation was inhibited in the parental PC9-ffluc cell line but not in the three resistant cell lines. Consistently, *EGFR* knockdown using specific siRNAs inhibited the viability of the parental PC9-ffluc cell line but not of the three resistant cell lines (Figure 1C). Although acquisition of an *EGFR*-C797S mutation has been reported as a mechanism of osimertinib resistance,[5] we did not detect this mutation in the parental PC9-ffluc cell line or in the three resistant cell lines. Additionally, the resistant cell lines maintained the *EGFR* exon-19 deletion present in the PC9-ffluc cells (Table 1).

3.2 | Detection of *KRAS*-G12V in the PC9-OR#2 cell line

To elucidate the resistance mechanism, we first examined whether an alternative receptor tyrosine kinase was activated in the resistant

TABLE 1 Analysis of mutations in *EGFR* and *KRAS* gene

Cells	EGFR			KRAS
	Exon-19 deletion	T790M	C797S	
PC9-ffluc	+	-	-	-
PC9-OR#1	+	-	-	-
PC9-OR#2	+	-	-	35G>T (G12V)
PC9-OR#3	+	-	-	-

cells. We observed that fibroblast growth factor receptor 3 (FGFR3) phosphorylation was enhanced in PC9-OR#1 and PC9-OR#2 cells (Figure 2A); however, combined treatment with osimertinib and the FGFR inhibitor infigratinib marginally inhibited the cell growth rate (Figure S1A). Moreover, MET and HER2[15] were activated in the PC9-OR#1 cells (Figure 2B). Therefore, we treated the cells with a MET inhibitor (crizotinib or capmatinib) or a HER2 inhibitor (afatinib) in combination with osimertinib. Crizotinib or capmatinib slightly sensitized PC9-OR#1 or PC9-OR#3 cells to osimertinib but did not sensitize PC9-OR#2 cells (Figure 2C). Additionally, afatinib did not suppress the growth of any of the resistant cell lines (Figure S1B). We previously reported that EMT occurs through a mechanism of acquired resistance to EGFR-TKIs[11] and anaplastic lymphoma kinase (ALK)-TKIs.[10] However, the expression of the epithelial marker E-cadherin did not decrease in the resistant cell lines, and the expression of the mesenchymal marker vimentin did not increase, indicating that EMT was not induced (Figure 2B). Thus, to further elucidate whether these resistant cells acquired gene mutations or gene amplifications, we isolated their genomic DNA and analyzed 409 cancer-associated genes using the Ion AmpliSeq Comprehensive Cancer Panel. Interestingly, a *KRAS* codon-35G>T missense mutation (G12V) was detected in PC9-OR#2 cells but not in the PC9-ffluc parental cells or in PC9-OR#1 or PC9-OR#3 cells (Figure 2D). Point mutations in the G12 codon of *KRAS* were reported by the FLAURA study as an acquired resistance mechanism in response to treatment with first-line osimertinib.[6] *KRAS*-G12V can cause constitutive activation of the RAS signaling pathway because mutant KRAS proteins bound to GTP (Guanosine triphosphate) are unable to return to the inactive form.[16] Consistently, RAS-GTP interaction was higher in PC9-OR#2 cells than that in PC9-ffluc parental cells (Figure S2A). Other known mutations or amplifications associated with osimertinib resistance were not detected in PC9-OR#2 cells. Furthermore, there were no mutations previously reported as associated with osimertinib resistance mechanisms in PC9-OR#1 or PC9-OR#3 cells according to analyses using the Ion AmpliSeq Comprehensive Cancer Panel, suggesting that an unknown mechanism could be associated with the resistance in these cell lines.

3.3 | *KRAS*-G12V drives osimertinib resistance in a clonal cell line derived from PC9-OR#2 cells

To elucidate whether *KRAS*-G12V could drive osimertinib resistance, we performed cell sorting to obtain clonal cell lines from the PC9-OR#2 cells, which contained *KRAS*-G12V at a high frequency. After establishing the resistant clone cell lines, we screened *KRAS*-G12V–positive cells based on the ratio of *KRAS*-G12V to wild-type *KRAS* using ddPCR. Clones #26, #31, and #33 showed a *KRAS*-G12V mutation frequency of >44.7%, indicating that ~90% of the clonal cells harbored *KRAS*-G12V (Figure 3A). Additionally, we confirmed that these clonal cell lines maintained the parental *EGFR* exon-19 deletion. To elucidate the effect of *KRAS*-G12V on acquired osimertinib resistance, we examined the sensitivity of each clone to osimertinib. Osimertinib resistance was >200-fold greater in the three clonal cell lines than in the parental PC9-ffluc cell line (Figure 3B).

Furthermore, to clarify whether the *KRAS* mutation contributed to osimertinib resistance, we knocked down *KRAS* expression using siKRAS. We found that knocking down *KRAS* in combination with osimertinib treatment significantly inhibited the viability of each clonal cell line (Figure 3C,D). Furthermore, we found that apoptosis markers, such as cleaved poly(ADP-ribose) polymerase and c-caspase-3, were detected only when *KRAS* knockdown was combined with osimertinib treatment for 72 hours (Figure 3E). Similar results were observed in PC9-OR#2 bulk cells (Figure S2B-D). Although HER2 expression was increased in these three cell clones, afatinib in combination with osimertinib did not decrease their cell viability. Moreover, the FGFR inhibitor infigratinib did not suppress cell viability, suggesting that bypass signaling was not associated with the osimertinib resistance in these three cell clones. To further elucidate whether expression of an activated *KRAS* allele could contribute to osimertinib resistance, we stably transfected PC9-ffluc cells and H1975 cells with *KRAS*-G12V. PC9-ffluc and H1975 stably expressing *KRAS*-G12V were selected by treating the cells with hygromycinB for 2 weeks. The PC9-ffluc-*KRAS*-G12V cells showed ~150-fold greater osimertinib resistance than the parental PC9-ffluc cells, and the H1975-*KRAS*-G12V cells showed ~200-fold greater osimertinib resistance than the parental H1975 cells (Figure 4A,B). Furthermore, *KRAS*-G12V expression in PC9-ffluc cells resulted in sustained ERK phosphorylation, even after osimertinib treatment (Figure 4C).

3.4 | Trametinib overcomes *KRAS*-G12V–induced osimertinib resistance

To investigate the role of mitogen-activated protein kinase (MAPK) signaling in inducing resistance in PC9-*KRAS*-G12V cells, we treated the cells with both osimertinib and trametinib. Trametinib monotherapy decreased cell growth by 50%, and combinatorial treatment showed additional efficacy (Figure 4D). Consistently, osimertinib partially inhibited ERK signaling, which was strongly suppressed in the presence of trametinib (Figure 4E). Similar results were observed in H1975-*KRAS*-G12V cells (Figure S4A,B).

We then investigated the effect of trametinib on the PC9-OR#2 *KRAS* mutant–positive clonal cell lines. Trametinib monotherapy reduced the growth of clones #26 and #33 by 40% and the growth of clone #31 by 60% (Figure 5A,B). Furthermore, combinatorial treatment with trametinib and osimertinib markedly reduced the growth

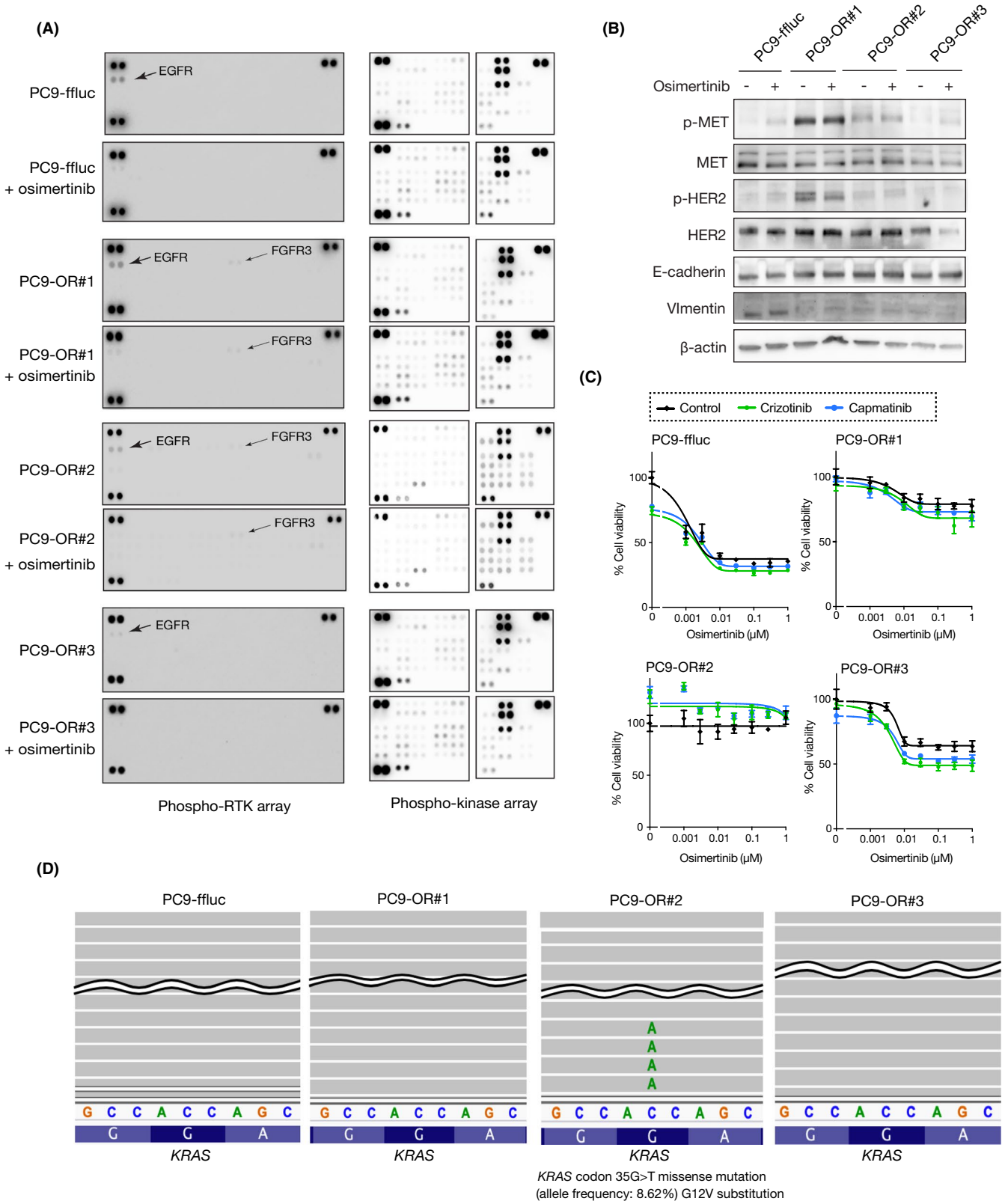

FIGURE 2 Analysis of the resistance mechanism in the generated cells. A, Parental PC9-ffluc cells and osimertinib-resistant cells were treated with 1 μM osimertinib for 72 h. Cell lysates from each cell line were analyzed using a phospho-RTK array kit. B, The parental PC9-ffluc cells and the resistant clones were treated with 1 μM osimertinib for 2 h. Changes in the phosphorylation levels of the indicated proteins were analyzed by Western blotting. C, MTT assays were performed to assess the growth inhibition of PC9-ffluc cells and the resistant clones, following osimertinib treatment in combination with 1 μM crizotinib for 72 h (n = 3). D, Genomic DNA was isolated from the parental PC9-ffluc cells and the resistant cells, and mutations in 409 cancer-associated genes were analyzed using the Ion AmpliSeq Comprehensive Cancer Panel. A Kirsten rat sarcoma *(KRAS)* codon 35G>T missense mutation (G12V) was detected in clone PC9-OR#2

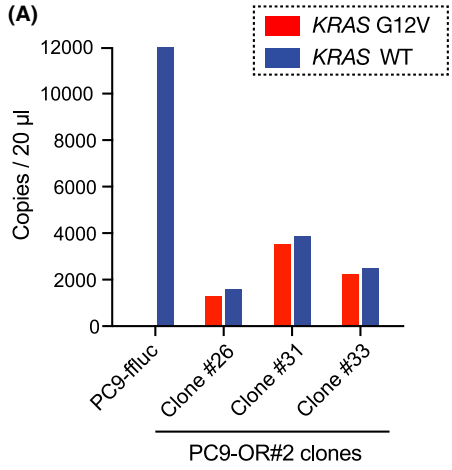

	KRAS	mutation ratio (%)	EGFR
PC9-ffluc	-	-	Exon-19 deletion
Clone #26	G12V	44.7	Exon-19 deletion
Clone #31	G12V	47.6	Exon-19 deletion
Clone #33	G12V	47.0	Exon-19 deletion

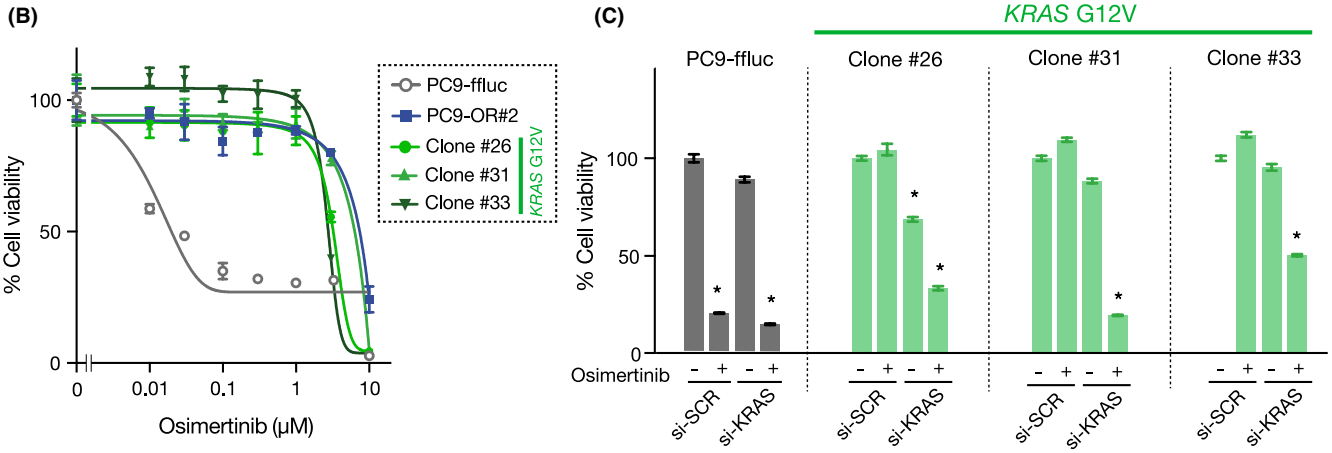

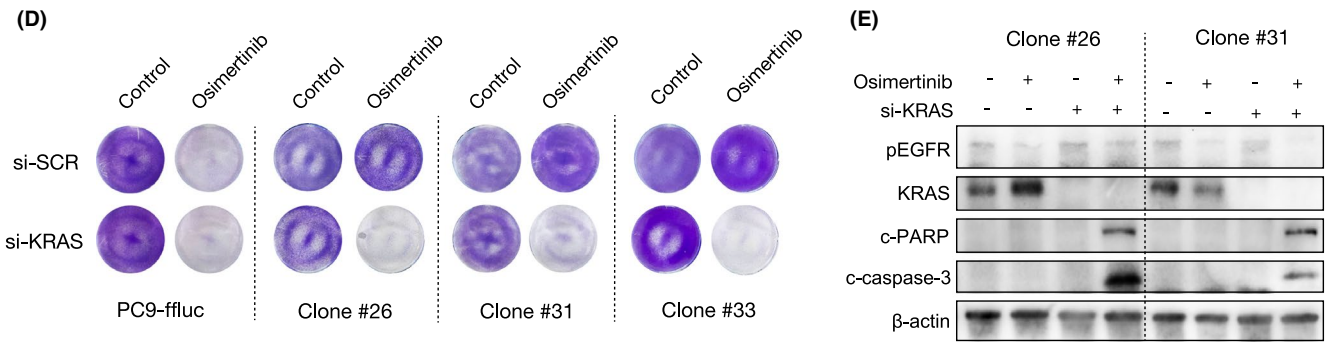

FIGURE 3 Analysis of Kirsten rat sarcoma *(KRAS)*-G12V–mutated clonal cell lines. A, Copy numbers of *KRAS*-G12V in parental PC9-ffluc cells and osimertinib-resistant PC9-OR#2 cells were evaluated to determine the *KRAS*-G12V mutation ratio by ddPCR. B, MTT assays were performed to assess the growth inhibition of PC9-ffluc cells, PC9-OR#2 cells, and the resistant clones, after osimertinib treatment for 72 h (n = 3). C, D, Control and KRAS siRNAs were transfected into parental PC9-ffluc cells and osimertinib-resistant OR#2 cells. At 24 h post transfection, the cells were treated with 1 µM osimertinib, and cell viabilities were measured after 72 h by performing MTT assays (n = 3) (C); after 1 wk, the cells were stained with crystal violet and examined visually (D). Error bars represent the SEM (D). *$P < .0001$. E, Control and KRAS siRNAs were transfected into the resistant clonal cell lines. At 24 h post transfection, the cells were treated with 1 µM osimertinib for 72 h, after which cell lysates were obtained and analyzed by immunoblotting with the indicated antibodies

of all three clonal cell lines. Additionally, we stained these clonal cell lines after treating them with trametinib and/or osimertinib for 1 week, which revealed the potent efficacy of combinatorial treatment in all three cell lines (Figure 5C). Moreover, after combined treatment with trametinib and osimertinib for 72 hours, we confirmed the expression of the apoptosis marker c-caspase-3 by Western blotting (Figure 5D) and immunofluorescence (Figure 5E) analyses.

3.5 | Combined treatment with trametinib overcomes osimertinib resistance in a mouse model of LMC

We then assessed the efficacy of combined treatment with osimertinib and trametinib in the mouse model of LMC. We first injected PC9-OR#2 clone #31 into the leptomeningeal space in SCID mice

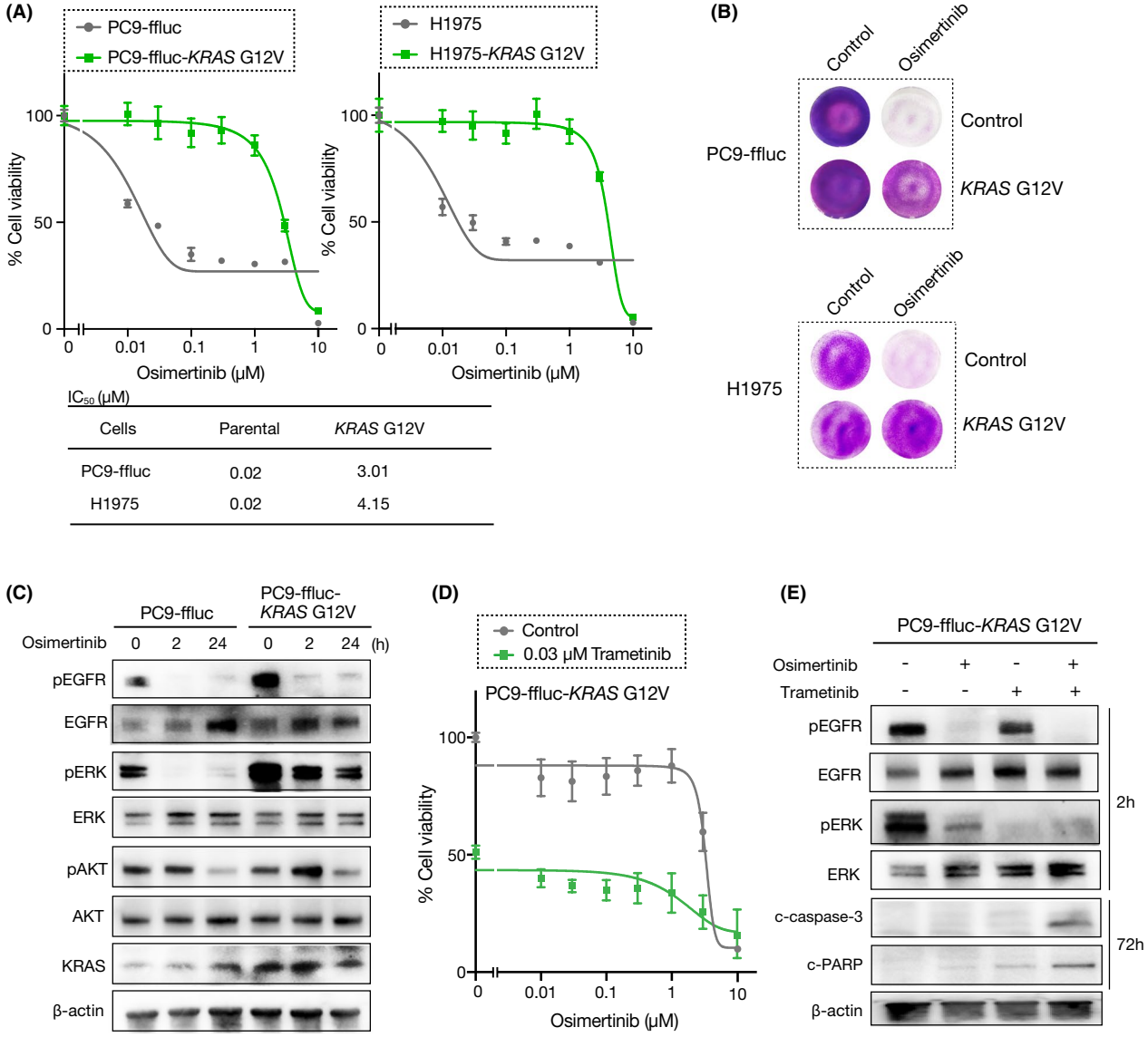

IC_{50} (μM)

Cells	Parental	*KRAS* G12V
PC9-ffluc	0.02	3.01
H1975	0.02	4.15

FIGURE 4 Analysis of non–small cell lung cancer NSCLC) cells stably expressing Kirsten rat sarcoma *(KRAS)*-G12V. A, MTT assays were performed to assess the growth inhibition of PC9-ffluc, PC9-ffluc-*KRAS*-G12V, H1975, and H1975-*KRAS*-G12V cells by osimertinib treatment for 72 h (n = 3). The calculated IC_{50} values are shown. The results are expressed as the mean ± SEM. B, PC9-ffluc, PC9-ffluc-*KRAS*-G12V, H1975, and H1975-*KRAS*-G12V were treated with osimertinib for 1 wk, followed by staining with crystal violet and visual examination. C, PC9-ffluc and PC9-ffluc-*KRAS*-G12V cells were treated with 1 μM osimertinib for 2 or 24 h. Changes in the phosphorylation levels of the indicated proteins were assessed by Western blotting. D, MTT assays were performed to assess the growth inhibition of PC9-*KRAS*-G12V cells treated with increasing concentration of osimertinib in combination with 0.03 μM trametinib for 72 h (n = 3). E, PC9-ffluc-*KRAS*-G12V cells were treated with 1 μM osimertinib and/or 0.03 μM trametinib for 2 or 72 h. Changes in the expression of the indicated proteins were evaluated by Western blotting

and then started treatment at 8 days post injection (oral administration of trametinib [0.6 mg/kg] and/or osimertinib [25 mg/kg]). The results showed that osimertinib delayed LMC progression for 3 weeks, whereas trametinib did not (Figure 6A). Moreover, combinatorial treatment with osimertinib and trametinib significantly prevented LMC progression for >5 weeks (Figure 6A,B). Similar results were observed in the mouse LMC model using PC9-OR#2 bulk cells (Figure S6A,B). Furthermore, the treatments caused no obvious systemic toxicity, as assessed by weight loss (Figure 6C). After 4 days of treatment, we stained the cancer cells with hematoxylin and eosin (H&E) and performed luciferase staining. Luciferase-positive cells were detected in untreated mice but hardly detected in stained cells because of the combination treatment (Figure S7).

4 | DISCUSSION

In this study, we identified *KRAS*-G12V in osimertinib-treated LMC derived from NSCLC with an *EGFR* mutation and determined that this mutation predominantly drove osimertinib resistance. Importantly,

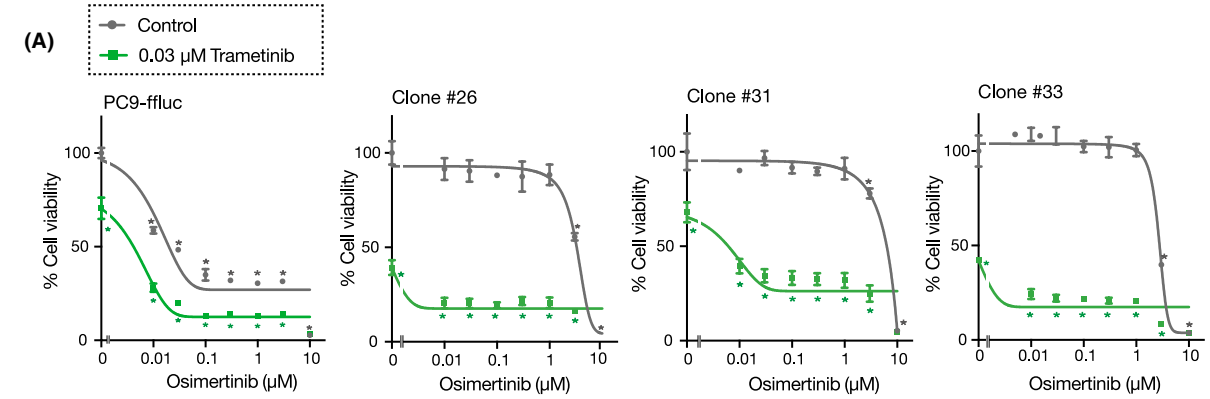

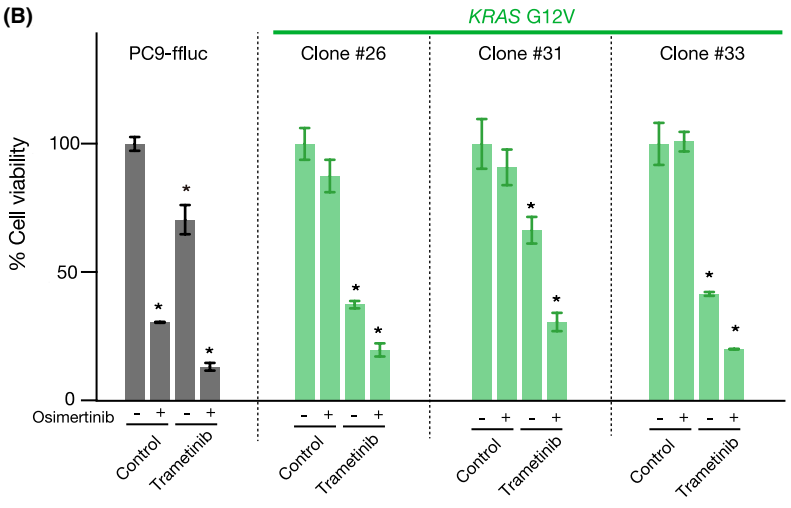

IC_{50} (μM)

	Osimertinib	+0.03 μM Trametinib
PC9-ffluc	0.02	<0.01
Clone #26	3.33	<0.01
Clone #31	6.53	<0.01
Clone #33	2.87	<0.01

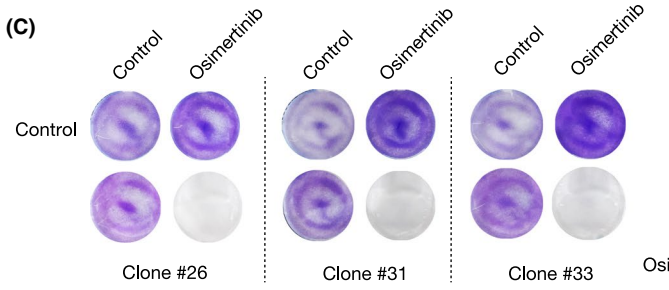

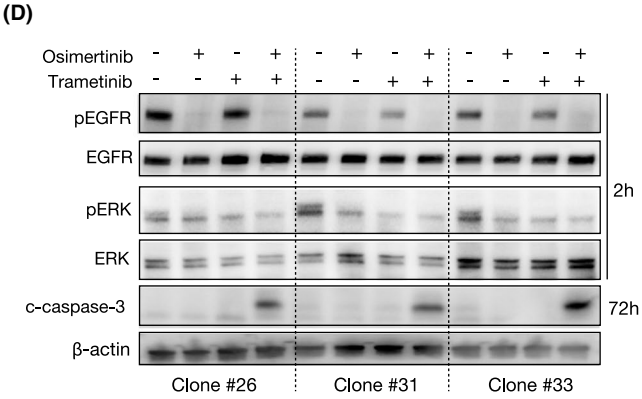

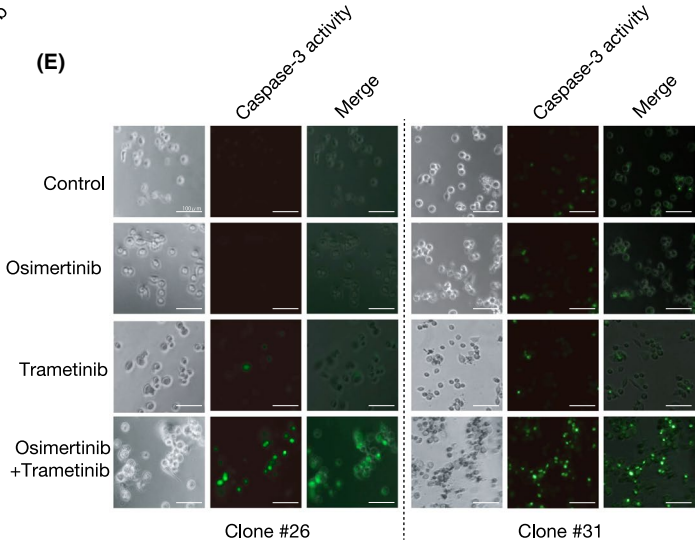

FIGURE 5 Effects of trametinib on Kirsten rat sarcoma *(KRAS)*-G12V–induced osimertinib resistance. A, B, MTT assays were performed to assess the growth inhibitory effects of combined treatment for 72 h (trametinib (0.03 μM) and increasing osimertinib concentrations) on PC9-OR#2 *KRAS*-positive clonal cell lines (n = 3). The calculated IC_{50} values are shown. The results are expressed as the mean ± SEM. C, PC9-OR#2 *KRAS* mutant–positive clonal cell lines were treated with 1 μM osimertinib in combination with 0.03 μM trametinib for 1 wk, followed by staining with crystal violet and visual examination. D, PC9-OR#2 *KRAS* mutant–positive clonal cell lines were treated with 1 μM osimertinib and/or 0.03 μM trametinib for 2 or 72 h. Changes in the expression of the indicated proteins were assessed by Western blotting. E, Clone #26 and clone #31 were treated with 1 μM osimertinib and/or 0.03 μM trametinib for 24 h. C-caspase-3 activity was measured using immunofluorescence

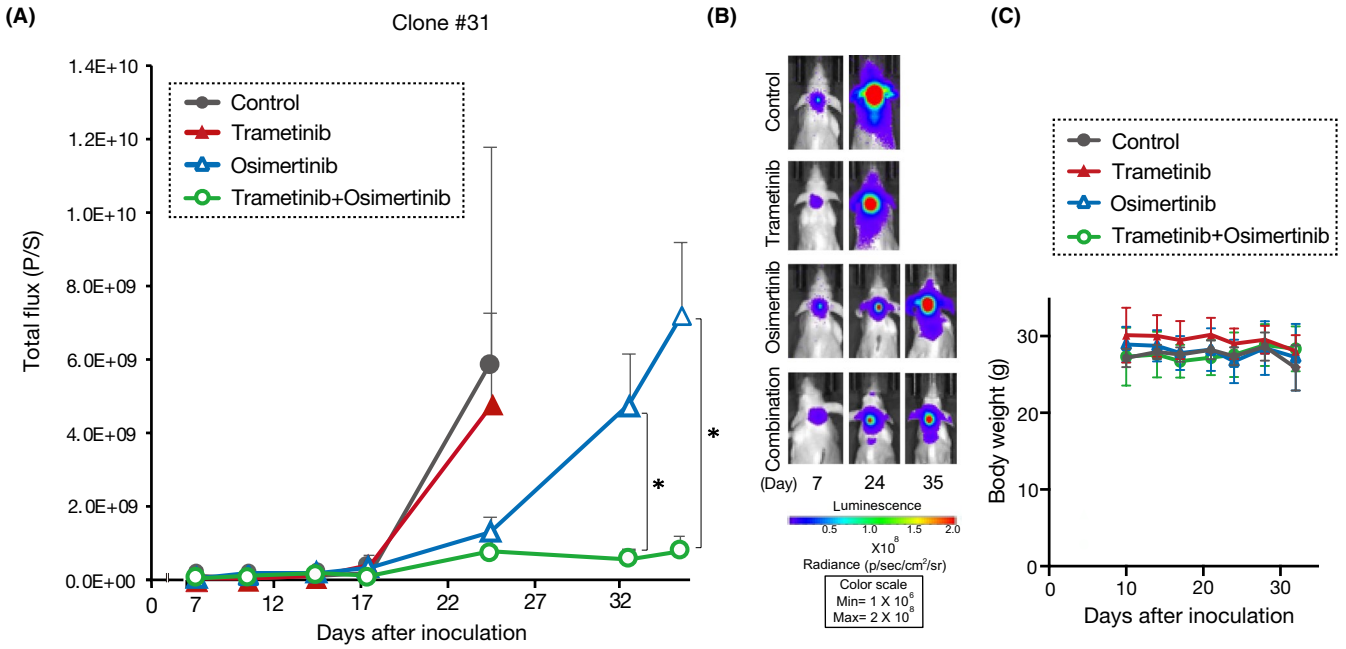

FIGURE 6 The effects of trametinib on osimertinib resistance in a mouse model of leptomeningeal carcinomatosis (LMC). A, PC9-OR#2 Kirsten rat sarcoma *(KRAS)* mutant–positive clonal cell line clone #31 (4×10^5 cells/0.1 mL) was injected in the leptomeningeal space of SHO-SCID mice (n = 15). Beginning on day 8, the mice were orally administered osimertinib (25 mg/kg) and trametinib (0.6 mg/kg) every day depending on the group; the mice were randomized into four groups (control group, n = 4; trametinib group, n = 4; osimertinib group, n = 4; combination treatment group; n = 3). Luminescence was measured twice per week until the experiment was terminated. The error bars represent the SEM. Two-sided Student's *t*-test was used for comparisons between two groups. The threshold for significance was designated as $P < .05$, when compared with the combination treatment group. B, Representative luminescence images in mice and fluorescence in the brain lesions are shown C, Time course of mouse body weight.

combinatorial treatment with trametinib and osimertinib circumvented resistance originating from *KRAS*-G12V in LMC with *EGFR*-mutant lung cancer cells both in vitro and in vivo.

The FLAURA study[6] revealed several plausible acquired resistance mechanisms to first-line osimertinib therapy, including alterations, such as *EGFR*-C797X (7%), loss of T790M, *MET* amplification (15%), *HER2* amplification (2%), *PIK3CA* mutations (7%), *BRAF* mutations (3%), and *KRAS* mutations (3%). These alterations occurred in patients with locally advanced or metastatic NSCLC with *EGFR*-mutated tumors. Further, *KRAS*-G12C accompanied with *MET* amplification occurred in one patient, and *KRAS*-G12D accompanied with *EGFR* C797X/L718Q mutations occurred in another patient. In the AURA study, *KRAS*-G12S mutation was accompanied by *EGFR*-C797S in a patient treated with first-line osimertinib. Moreover, in the AURA3 study, a patient with *EGFR* T790M–positive advanced NSCLC harbored *KRAS*-G12D accompanied by both *MET* amplification and *EGFR*-C797X. Thus, *KRAS*-G12 might be acquired following osimertinib treatment; however, it remains unclear whether any *KRAS*-G12 mutations cause osimertinib resistance because all patients with *KRAS* mutations also display other candidate resistance mechanisms, such as *EGFR* mutation and/or *MET* amplification.

Here, we isolated *EGFR*-mutant lung cancer clonal cell lines with a high frequency of *KRAS*-G12V and analyzed osimertinib resistance. We isolated clonal cell lines with ~200-fold greater osimertinib resistance than that of the parental cell line and showed that knocking down *KRAS* expression sensitized the clones to osimertinib. Additionally, transfection of *KRAS*-G12V in *EGFR*-mutant PC9 and H1975 cells conferred osimertinib resistance. To the best of our knowledge, this is the first report demonstrating the dominant role of *KRAS*-G12V in osimertinib resistance in *EGFR*-mutant NSCLC. In most PC9-OR#2 cells, *KRAS* knockdown or trametinib treatment suppressed cell viability. These results imply that clonal cells expressing *KRAS*-G12V might dominate the resistance status, although this possibility requires further confirmation.

Notably, *KRAS*-G12V conferred osimertinib resistance independent of EGFR activity. *KRAS*-G12 mutations are predominant in human cancers, with a relative frequency of 89%, as compared with *KRAS*-G13 mutations (9%) and *KRAS*-Q61 mutations (1%).[16] *KRAS* mutations are considered oncogenic drivers in patients with advanced NSCLC. Point mutations in the G12 codon of *KRAS* can cause constitutive activation of the RAS signaling pathway by locking mutant KRAS proteins in the GTP-bound conformation.[16] In the present study, we found that RAS-GTP interaction was higher in osimertinib-resistant *KRAS*-G12V–positive cells and observed increased levels of phospho-ERK, which can be triggered by RAS activation.[17] RAS-MAPK signaling can play important roles in EGFR-TKI resistance. Alternative mechanisms of EGFR-TKI resistance development in *EGFR*-mutant lung cancer are associated with increased dependency on RAS-MAPK signaling, including loss of neurofibromin 1, *CRKL* amplification, and EMT.[18-20] In colorectal cancer, mutations in *KRAS*, *NRAS*, and *BRAF* are associated with cetuximab resistance.[21] Collectively, our data suggest that

KRAS activation serves as an alternative bypass pathway to circumvent blockage of EGFR-dependent survival signaling caused by osimertinib.

Recent data from clinical trials show the excellent efficacy of EGFR-TKIs against CNS metastasis of *EGFR*-mutant NSCLC. Erlotinib and gefitinib showed efficacy against TKI-naive CNS metastases of *EGFR*-mutated lung cancer.[22,23] Notably, in patients harboring *EGFR*-mutated lung cancer with CNS metastasis, osimertinib penetrated the CNS more efficiently and demonstrated better clinical efficacy than first-generation EGFR-TKIs.[6,24] We previously reported that osimertinib was well distributed in leptomeningeal metastatic tumor lesions compared with the nontumoral cerebral parenchyma in a mouse model of LMC.[25] Further, we reported an increased *MET* copy number in a gefitinib-resistant LMC model of *EGFR*-mutated lung cancer cells, whereas the *EGFR*-T790M mutation was detected in gefitinib-resistant extra-CNS lesions.[26] However, in the present study, we detected neither an increase in *MET* copy number nor secondary *EGFR* mutations. These results imply that *KRAS* mutations might occur specifically in osimertinib-treated LMC.

Trametinib is a selective inhibitor of MEK1/MEK2, which is the only known substrate of the BRAF kinase in the MAPK pathway. Treatment with dabrafenib and trametinib has been approved for patients with metastatic NSCLC harboring *BRAF* V600E mutations.[27] In a recent study on pediatric patients with glioma or CNS tumors with MAPK pathway mutations, the patients received trametinib alone (n = 9) or in combination with another antineoplastic agent (n = 5). Although five patients showed a partial response, four retained the disease, indicating that trametinib was capable of penetrating into the CNS and that trametinib-based therapy could be effective against MAPK-driven CNS tumors.[28] In the present study, we observed that trametinib was distributed in leptomeningeal metastatic tumor lesions and controlled osimertinib-resistant LMC (Figure 6A). Although patients with MAPK-activated myeloma treated with trametinib exhibit several types of toxicity,[29] we found that trametinib caused no obvious systemic toxicity, even when administered in combination with osimertinib. These data suggest that trametinib might be suitable for combinatorial use with osimertinib. Future clinical trials are necessary to fully elucidate the safety and efficacy of combinatorial treatment with osimertinib and trametinib against EGFR-TKI–refractory LMC with *KRAS*-G12V mutation.

In conclusion, we showed that *KRAS*-G12V–driven *EGFR*-mutant lung cancer cells acquired resistance to osimertinib in the leptomeningeal space. Moreover, combinatorial treatment with osimertinib and trametinib overcame resistance in our mouse model of LMC. These findings provide a rationale for initiating clinical trials to investigate the effects of novel therapies targeting both EGFR and MEK in *EGFR*-mutated NSCLC with osimertinib-resistant LMC.

ACKNOWLEDGMENTS

This work was supported by the JSPS KAKENHI (grant numbers: 17K09649, Shinji Takeuchi; 18K07261, Koji Fukuda; 20K17213, Sakiko Otani; 19H03665, Seiji Yano).

DISCLOSURE

Seiji Yano received speaking fees from Pfizer and Chugai Pharmaceutical Co., Ltd., as well as a research grant from Chugai Pharmaceutical Co., Ltd. The other authors have nothing to disclose.

ORCID

Koji Fukuda https://orcid.org/0000-0001-8544-6244
Akihiro Nishiyama https://orcid.org/0000-0002-4805-9787
Seiji Yano https://orcid.org/0000-0002-6151-2988

REFERENCES

1. Barnholtz-Sloan JS, Sloan AE, Davis FG, Vigneau FD, Lai P, Sawaya RE. Incidence proportions of brain metastases in patients diagnosed (1973 to 2001) in the Metropolitan Detroit Cancer Surveillance System. *J Clin Oncol*. 2004;22:2865-2872.
2. Iuchi T, Shingyoji M, Itakura M, et al. Frequency of brain metastases in non-small-cell lung cancer, and their association with epidermal growth factor receptor mutations. *Int J Clin Oncol*. 2015;20:674-679.
3. Li YS, Jiang BY, Yang JJ, et al. Leptomeningeal metastases in patients with NSCLC with EGFR mutations. *J Thorac Oncol*. 2016;11:1962-1969.
4. Rosell R, Carcereny E, Gervais R, et al. Erlotinib versus standard chemotherapy as first-line treatment for European patients with advanced EGFR mutation-positive non-small-cell lung cancer (EURTAC): a multicentre, open-label, randomised phase 3 trial. *Lancet Oncol*. 2012;13:239-246.
5. Minari R, Bordi P, Tiseo M. Third-generation epidermal growth factor receptor-tyrosine kinase inhibitors in T790M-positive non-small cell lung cancer: review on emerged mechanisms of resistance. *Transl Lung Cancer Res*. 2016;5:695-708.
6. Soria JC, Ohe Y, Vansteenkiste J, et al. Osimertinib in untreated EGFR-mutated advanced non-small-cell lung cancer. *N Engl J Med*. 2018;378:113-125.
7. Erickson AW, Brastianos PK, Das S. Assessment of effectiveness and safety of osimertinib for patients with intracranial metastatic disease: a systematic review and meta-analysis. *JAMA Netw Open*. 2020;3:e201617.
8. Ahluwalia MS, Becker K, Levy BP. Epidermal growth factor receptor tyrosine kinase inhibitors for central nervous system metastases from non-small cell lung cancer. *Oncologist*. 2018;23:1199-1209.
9. Arulananda S, Do H, Rivalland G, et al. Standard dose osimertinib for erlotinib refractory T790M-negative EGFR-mutant non-small cell lung cancer with leptomeningeal disease. *J Thorac Dis*. 2019;11:1756-1764.
10. Fukuda K, Takeuchi S, Arai S, et al. Epithelial-to-mesenchymal transition is a mechanism of ALK inhibitor resistance in lung cancer independent of ALK mutation status. *Cancer Res*. 2019;79:1658-1670.
11. Fukuda K, Takeuchi S, Arai S, et al. GSK-3 inhibition overcomes EMT-associated resistance to osimertinib in EGFR mutant lung cancer. *Cancer Sci*. 2020;111:2374-2384.
12. Miyazawa H, Tanaka T, Nagai Y, et al. Peptide nucleic acid-locked nucleic acid polymerase chain reaction clamp-based detection test for gefitinib-refractory T790M epidermal growth factor receptor mutation. *Cancer Sci*. 2008;99:595-600.
13. Balak MN, Gong Y, Riely GJ, et al. Novel D761Y and common secondary T790M mutations in epidermal growth factor receptor-mutant lung adenocarcinomas with acquired resistance to kinase inhibitors. *Clin Cancer Res*. 2006;12:6494-6501.
14. Taniguchi H, Takeuchi S, Fukuda K, et al. Amphiregulin triggered epidermal growth factor receptor activation confers in vivo crizotinib-resistance of EML4-ALK lung cancer and circumvention by epidermal growth factor receptor inhibitors. *Cancer Sci*. 2017;108:53-60.

15. Planchard D, Loriot Y, André F, et al. EGFR-independent mechanisms of acquired resistance to AZD9291 in EGFR T790M-positive NSCLC patients. *Ann Oncol*. 2015;26:2073-2078.
16. Lu S, Jang H, Muratcioglu S, et al. Ras conformational ensembles, allostery, and signaling. *Chem Rev*. 2016;116:6607-6665.
17. Yaeger R, Corcoran RB. Targeting alterations in the RAF-MEK pathway. *Cancer Discov*. 2019;9:329-341.
18. Huang MH, Lee JH, Chang YJ, et al. MEK inhibitors reverse resistance in epidermal growth factor receptor mutation lung cancer cells with acquired resistance to gefitinib. *Mol Oncol*. 2013;7:112-120.
19. Buonato JM, Lazzara MJ. ERK1/2 blockade prevents epithelial-mesenchymal transition in lung cancer cells and promotes their sensitivity to EGFR inhibition. *Cancer Res*. 2014;74:309-319.
20. Cheung HW, Du J, Boehm JS, et al. Amplification of CRKL induces transformation and epidermal growth factor receptor inhibitor resistance in human non-small cell lung cancers. *Cancer Discov*. 2011;1:608-625.
21. Misale S, Arena S, Lamba S, et al. Blockade of EGFR and MEK intercepts heterogeneous mechanisms of acquired resistance to anti-EGFR therapies in colorectal cancer. *Sci Transl Med*. 2014;6:224ra226.
22. Namba Y, Kijima T, Yokota S, et al. Gefitinib in patients with brain metastases from non-small-cell lung cancer: review of 15 clinical cases. *Clin Lung Cancer*. 2004;6:123-128.
23. Yi HG, Kim HJ, Kim YJ, et al. Epidermal growth factor receptor (EGFR) tyrosine kinase inhibitors (TKIs) are effective for leptomeningeal metastasis from non-small cell lung cancer patients with sensitive EGFR mutation or other predictive factors of good response for EGFR TKI. *Lung Cancer*. 2009;65:80-84.
24. Ballard P, Yates JW, Yang Z, et al. Preclinical comparison of osimertinib with other EGFR-TKIs in EGFR-mutant NSCLC brain metastases models, and early evidence of clinical brain metastases activity. *Clin Cancer Res*. 2016;22:5130-5140.
25. Arai S, Takeuchi S, Fukuda K, et al. Osimertinib overcomes alectinib resistance caused by amphiregulin in a leptomeningeal carcinomatosis model of ALK-rearranged lung cancer. *J Thorac Oncol*. 2020;15:752-765.
26. Nanjo S, Arai S, Wang W, et al. MET copy number gain is associated with gefitinib resistance in leptomeningeal carcinomatosis of EGFR-mutant lung cancer. *Mol Cancer Ther*. 2017;16:506-515.
27. Odogwu L, Mathieu L, Blumenthal G, et al. FDA approval summary: dabrafenib and trametinib for the treatment of metastatic non-small cell lung cancers harboring BRAF V600E mutations. *Oncologist*. 2018;23:740-745.
28. Paul MR, Pehlivan KC, Milburn M, Yeh-Nayre L, Elster J, Crawford JR. Trametinib-based treatment of pediatric CNS tumors: a single institutional experience. *J Pediatr Hematol Oncol*. 2020;42:e730-e737.
29. Heuck CJ, Jethava Y, Khan R, et al. Inhibiting MEK in MAPK pathway-activated myeloma. *Leukemia*. 2016;30:976-980.

SUPPORTING INFORMATION

Additional supporting information may be found online in the Supporting Information section.

How to cite this article: Fukuda K, Otani S, Takeuchi S, et al. Trametinib overcomes *KRAS*-G12V–induced osimertinib resistance in a leptomeningeal carcinomatosis model of *EGFR*-mutant lung cancer. *Cancer Sci*. 2021;112:3784–3795. https://doi.org/10.1111/cas.15035